https://doi.org/10.5194/acp-2019-521
Preprint. Discussion started: 8 July 2019

Atmospheric Chemistry and Physics Discussions

A methodology to constrain carbon dioxide emissions from coal-fired power plants using satellite observations of co-emitted nitrogen dioxide

Fei Liu[1,2], Bryan N. Duncan[2], Nickolay A. Krotkov[2], Lok N. Lamsal[1,2], Steffen Beirle[3], Debora Griffin[4], Chris A. McLinden[4], Daniel L. Goldberg[5], and Zifeng Lu[5]

[1]Universities Space Research Association (USRA), Goddard Earth Sciences Technology and Research (GESTAR), Columbia, MD, USA
[2]Goddard Space Flight Center, Greenbelt, MD, USA
[3]Max-Planck-Institut für Chemie, Mainz, Germany
[4]Air Quality Research Division, Environment and Climate Change Canada, Toronto, ON, Canada
[5]Energy Systems Division, Argonne National Laboratory, Lemont, IL, USA

Correspondence to: Fei Liu (fei.liu@nasa.gov)

Abstract. We present a novel method to infer CO_2 emissions from individual power plants based on satellite observations of co-emitted nitrogen dioxide (NO_2) and demonstrate its utility on US power plants, where accurate stack emission estimates of both gases are available for comparison. In the first step of our methodology, we infer nitrogen oxides (NO_x) emissions from isolated power plants using Ozone Monitoring Instrument (OMI) NO_2 tropospheric vertical column densities (VCDs) averaged over the ozone season (May-September) and a "top-down" approach that we previously developed. Second, we determine the relationship between NO_x and CO_2 emissions based on the direct stack emissions measurements reported by continuous emissions monitoring system (CEMS) programs, accounting for coal type, boiler firing type, NO_x emission control device type, and changes in operating conditions. Third, we estimate CO_2 emissions of the ozone season for a plant using the OMI-estimated NO_x emissions and the CEMS NO_x/CO_2 emission ratio. We find that the CO_2 emissions estimated by our satellite-based method during 2005–2017 are in reasonable agreement with the CEMS measurements, with a relative difference of 8% ± 41% (mean ± standard deviation) for the selected US power plants in our analysis. Total uncertainty in the inferred CO_2 estimates is partly associated with the uncertainty associated with the OMI NO_2 VCD data, so we expect that it will decrease when our method is applied to OMI-like sensors with improved capabilities, such as TROPOspheric Monitoring Instrument (TROPOMI) and geostationary Tropospheric Emissions: Monitoring Pollution (TEMPO). The broader implication of our methodology is that it has the potential to provide an additional constraint on CO_2 emissions from power plants in regions of the world without reliable emissions accounting. We explore the feasibility by applying our methodology to a power plant in South Africa, where the satellite-based emission estimates show reasonable consistency with other estimates.

1 Introduction

Thermal power plants, particularly coal-fired power plants, are among the largest anthropogenic CO_2 emitters, contributing ~40% of energy-related CO_2 emissions globally in 2010 (Janssens-Maenhout et al., 2017). Coal-fired power plants are expected to be one of the primary contributors of CO_2 emissions in the coming decades because of abundant world coal reserves (Shindell and Faluvegi, 2010). Therefore, it is important to accurately monitor global CO_2 emissions from power production in order to better predict climate change (Shindell and Faluvegi, 2010) and to support the development of effective climate mitigation strategies.

CO_2 emissions from power plants are typically quantified based on bottom-up approaches using fuel consumption and fuel quality, though fuel properties are not always well known, resulting in uncertainties in the estimated CO_2 emissions for

https://doi.org/10.5194/acp-2019-521
Preprint. Discussion started: 8 July 2019

Atmospheric Chemistry and Physics Discussions

individual plants (Wheeler and Ummel, 2008). Even for US power plants that are considered to have the most accurate information on fuel usage among world nations, the difference between emissions estimated based on fuel usage and those reported as part of continuous emissions monitoring systems (CEMS) programs is typically about 20% (Ackermann and Sundquist, 2008). Thus, emission estimates based on independent data sources such as satellite observations are a desirable complement to validate and improve the current CO_2 emissions inventories, especially in countries without CEMS data, which is the case in most of the world.

Anthropogenic CO_2 emissions have been estimated from space-based CO_2 observations, but the existing satellite CO_2 sensors are designed to provide constraints on natural CO_2 sources and sinks (Basu et al., 2013; Houweling et al, 2015), and thus their capability for monitoring anthropogenic point sources is limited (Nassar et al., 2017). Observations from sensors, including the Scanning Imaging Absorption Spectrometer for Atmospheric Chartography (SCIAMACHY; Burrows et al., 1995), Greenhouse gases Observing SATellite (GOSAT; Yokota et al., 2009), and Orbiting Carbon Observatory-2 (OCO-2; Crisp et al., 2015), show statistically significant enhancements over metropolitan regions (Kort et al., 2012; Schneising et al., 2013; Janardanan et al., 2016; Buchwitz et al., 2018; Reuter et al., 2019). However, very few studies have focused on individual point sources. Bovensmann et al. (2010) and Velazco et al. (2011) presented a promising satellite remote sensing concept to infer CO_2 emissions for power plants based on the atmospheric CO_2 column distribution. Nassar et al. (2017) and Reuter et al. (2019) presented the only quantification of CO_2 emissions from individual power plants using OCO-2 observations. However, due to the narrow swath of the OCO-2 sensor, their method cannot be currently applied to generate a global CO_2 emissions database.

In contrast to CO_2, inferring NO_x emissions from individual power plants using satellite NO_2 column retrievals has been done with a higher degree of confidence (e.g., Duncan et al., 2013; de Foy et al., 2015). The Dutch-Finnish Ozone Monitoring Instrument (OMI) on NASA's Earth Observing System Aura spacecraft (Schoeberl et al., 2006) provides daily, global NO_2 tropospheric vertical column densities (VCDs) at a spatial resolution of 13×24 km^2 (at nadir) (Levelt et al., 2006; 2018; Krotkov et al., 2017), which allows emission signals from individual power plants to be resolved. Beirle et al. (2011) first analyzed isolated large sources (i.e., megacities and the US Four Corners power plant) by averaging OMI NO_2 tropospheric VCDs separately for different wind directions, which allows to determine NO_x emissions and lifetimes by fitting an exponentially modified Gaussian function. Several follow-up studies (e.g., de Foy et al., 2015; Lu et al., 2015 and Goldberg et al., 2019) further developed this approach and inferred NO_x emissions from isolated power plants and cities. More recently, we advanced this approach for sources located in polluted areas to infer NO_x emissions for 17 power plants and 53 cities across China and the US (Liu et al., 2016; 2017).

Since NO_x is co-emitted with CO_2, NO_x emissions inferred from satellite data may be used to estimate CO_2 emissions from thermal power plants. Previous analyses estimated regional CO_2 emissions based on satellite-derived NO_x emissions and the NO_x to CO_2 emission ratios from bottom-up emission inventories (Berezin et al., 2013; Konovalov et al., 2016) or co-located satellite retrievals of CO_2 and NO_2 (Reuter et al., 2014). Hakkarainen et al. (2016) confirmed the spatial correlation between CO_2 spatial anomalies and OMI NO_2 VCD enhancements at the regional scale using satellite observations at higher resolution. More recently, the co-located regional enhancements of CO_2 observed by OCO-2 and NO_2 observed by TROPOMI were analysed to monitor localized CO_2 emissions (Reuter et al., 2019).

In this study, we present a novel method to estimate CO_2 emissions from individual power plants using OMI NO_2 observations and auxiliary CEMS information on NO_x to CO_2 emission ratios. We apply our approach to US power plants, which have an exceptionally detailed CEMS database, in order to validate our method. We discuss the uncertainties and limitations of our approach. Finally, we present the application of our method to power plants in South Africa. We discuss other potential applications in conclusion, including to other NO_2 datasets from new and upcoming satellite instruments.

https://doi.org/10.5194/acp-2019-521
Preprint. Discussion started: 8 July 2019

Atmospheric Chemistry and Physics Discussions

2 Method

In this section, we present a novel method to infer CO_2 emissions ($E_{CO_2}^{Sat}$) from satellite-derived NO_x emissions ($E_{NO_x}^{Sat}$) for individual coal-fired power plants using the following equation:

$$E_{CO_2,y}^{Sat} = \frac{E_{NO_x,y}^{Sat}}{ratio_{i,y}^{CEMS}}, \quad (1)$$

where *i* represents coal type and *y* represents the target year. We demonstrate our method on US power plants since there are accurate CEMS stack measurements of NO_x and CO_2 emissions with which to validate $E_{CO_2}^{Sat}$. In Section 2.1, we describe how to estimate $E_{NO_x}^{Sat}$ from OMI NO_2 tropospheric VCD observations. In Section 2.2, we discuss how to estimate the ratio of NO_x to CO_2 emissions ($ratio_y^{CEMS} = E_{NO_x,y}^{CEMS} / E_{CO_2,y}^{CEMS}$) from CEMS stack measurements in the US Emissions & Generation Resource Integrated Database (eGRID; USEPA, 2018). Since post-combustion NO_x control systems, including selective noncatalytic reduction (SNCR) and selective catalytic reduction (SCR), change the correlation between $E_{NO_x}^{CEMS}$ and $E_{CO_2}^{CEMS}$, we present separate methods to determine $ratio_y^{CEMS}$ for power plants without and with post-combustion NO_x control systems in Section 2.2.1 and Section 2.2.2, respectively. We discuss the validation of the estimated $E_{CO_2}^{Sat}$ in Section 3.

2.1 Estimating satellite-derived NO_x emissions ($E_{NO_x}^{Sat}$)

From all US coal-fired power plants, we selected 21 power plants for estimating $E_{NO_x}^{Sat}$. We chose these plants based on $E_{NO_x}^{CEMS}$ (i.e., > 10 Gg/yr in 2005) and relative isolation from other large sources and relative isolation from other large sources to avoid contamination of a power plant's NO_x plumes by NO_x from other sources. Power plants located in urban areas (i.e., within a radius of 100 km from city centers), or clustered in close proximity (i.e., 50 km) with other large industrial plants are excluded by visual inspection satellite imagery from Google Earth. The top 200 largest US cities (rank by 2018 population as estimated by the United States Census Bureau, available at https://en.wikipedia.org/wiki/List_of_United_States_cities_by_population) are used to select power plants.As discussed below, we are able to estimate $E_{NO_x}^{Sat}$ for 8 of the 21 plants. The locations of the 8 plants are shown in Figure 5.

We follow the method of Liu et al. (2016; 2017) to estimate $E_{NO_x}^{Sat}$ for 2005 to 2017. In our analysis, we use OMI NO_2 tropospheric VCDs from the NASA OMI standard product, version 3.1 (Krotkov et al., 2017) together with meteorological wind information from the Modern-Era Retrospective Analysis for Research and Applications, version 2 (MERRA-2; Gelaro et al., 2017). We only analyze the ozone season (May-September), in order to exclude winter data, which have larger uncertainties and longer NO_x lifetime. As in our previous study (Liu et al., 2017), we use the changes of VCDs under calm wind conditions (wind speed < 2 m/s below 500 m) and windy conditions (wind speed > 2 m/s) to fit the effective NO_x lifetime. We then estimate the average NO_2 total mass integrated around a power plant on the basis of the 3-year mean VCDs, in agreement with previous studies (Fioletov et al., 2011; Lu et al., 2015). The NO_2 total mass is scaled by a factor of 1.32 in order to derive total NO_x mass following Beirle et al. (2011). The NO/NO_2 ratio might differ locally in plumes, but the influence is not expected to be dramatic on the scales of the OMI footprint (at least 13 km×24 km), considering the overpass time of OMI close to noon, the selection of cloud-free observations, and the focus on the ozone season and polluted regions with generally high tropospheric ozone. The uncertainty associated with the NO/NO_2 ratio has been discussed in detail in Section 3 of the supplement in Liu et al. (2016). The 3-year average $E_{NO_x}^{Sat}$ is derived from the corresponding 3-year average NO_x mass divided by the average NO_x lifetime of the entire study period (Liu et al., 2017). Fitting results of insufficient quality (e.g., correlation coefficient of the fitted and observed NO_2 distributions <0.9) are excluded from this analysis, consistent with the criteria in Section 2.2 of Liu et al. (2016). This final filtering leaves 18 power plants, of which 8

https://doi.org/10.5194/acp-2019-521
Preprint. Discussion started: 8 July 2019

Atmospheric Chemistry and Physics Discussions

have valid results for all consecutive 3-year periods between 2005 and 2017. More details of the approach are documented in Liu et al. (2017).

We use the Rockport power plant (37.9 °N, 87.0 °W) in Indiana to demonstrate our approach. This power plant is particularly well suited for estimating $E_{NO_x}^{Sat}$, because it is a large and isolated NO_x point source. Figure 1 displays $E_{NO_x}^{Sat}$ based on 3-year mean VCDs. For simplicity, the 3-year period is represented by the middle year with an asterisk (e.g., 2006* denotes the period from 2005 to 2007). For comparison to $E_{NO_x}^{Sat}$, $E_{NO_x}^{CEMS}$ averaged over the period of May to September is derived from Air Markets Program Data (available at https://ampd.epa.gov/ampd/). For this particular plant, $E_{NO_x}^{Sat}$ and $E_{NO_x}^{CEMS}$ show positive biases (of varying magnitude) during the entire period, except the last two years. The coefficient of determination for the entire period is R^2=0.68. The relative differences for individual 3-year means (defined as $(E_{NO_x}^{Sat} - E_{NO_x}^{CEMS})/E_{NO_x}^{CEMS}$) range from -20% to 41%, because of the uncertainties of $E_{NO_x}^{Sat}$ as discussed in Section 3.2. Both datasets present a declining trend from 2012*. The total declines of 45% and 26% since 2012* in $E_{NO_x}^{Sat}$ and $E_{NO_x}^{CEMS}$ are attributed to the 25% decrease in net electricity generation for the plant. The average relative difference of $E_{NO_x}^{Sat}$ and $E_{NO_x}^{CEMS}$ for the 8 plants in this study is 0% ±33%, ranging from -58% to 72% for individual 3-year periods (Figure 5).

2.2 Estimating NO_x to CO_2 emission ratios using CEMS data ($ratio^{CEMS}$)

We determine the observed relationship between $E_{NO_x}^{CEMS}$ and $E_{CO_2}^{CEMS}$ for coal-fired power plants using eGRID information about each plant's net electric generation, boiler firing types (e.g., tangential or wall-fired boiler), NO_x control device type, fossil fuel type (with categories of coal, oil, gas and other), and coal type (with categories of bituminous, lignite, subbituminous, refined and waste coal). We only use data of power plants with more than 99% of the fuel burned being coal as reported in eGRID. We analyze the relationship between $E_{NO_x}^{CEMS}$ and $E_{CO_2}^{CEMS}$ by coal type, as emission characteristics vary widely by coal type.

eGRID includes two sets of emission data for NO_x and CO_2: 1) calculated from fuel consumption data and 2) observed by stack monitoring (i.e., $E_{NO_x}^{CEMS}$ and $E_{CO_2}^{CEMS}$). Here we focus on eGRID CEMS data as $E_{NO_x}^{CEMS}$ are reported to be highly accurate with an error of less than 5% (e.g., Glenn et al., 2003). $E_{CO_2}^{CEMS}$ may have larger uncertainties than fuel-based emissions estimates due to uncertainties in the calculation of flue gas flow (Majanne et al., 2015). Nevertheless, we use $E_{CO_2}^{CEMS}$ to relate NO_x emissions to CO_2 emissions, since the primary uncertainty of $E_{NO_x}^{CEMS}$ and $E_{CO_2}^{CEMS}$ arises from the calculation of the flue gas flow, which will cancel in $ratio^{CEMS}$.

2.2.1 Coal-fired power plants without post-combustion NO_x control systems

We first limited our analysis to $E_{NO_x}^{CEMS}$ and $E_{CO_2}^{CEMS}$ from coal-fired power plants without post-combustion NO_x control systems in operation in a given year (Table 1). We find that $E_{NO_x}^{CEMS}$ and $E_{CO_2}^{CEMS}$ have a strong linear relationship (Figure 2). In Figure 2a, we compare $E_{NO_x}^{CEMS}$ and $E_{CO_2}^{CEMS}$ from power plants (using bituminous coal) by boiler firing type in 2005. We use bituminous coal-fired plants for illustration, as bituminous coal is the most widely used coal in US power plants. We analyze power plants that use cyclone or cell burner boilers separately and exclude them in Figure 2 because they typically produce higher NO_x emissions than other boiler types (USEPA, 2009; available at https://www3.epa.gov/ttn/chief/ap42/ch01/index.html). A strong linear relationship between $E_{NO_x}^{CEMS}$ and $E_{CO_2}^{CEMS}$ is evident with excellent correlation (R^2= 0.93, N = 278), regardless of boiler firing types. Similar linear relationships exist for other years (e.g., year 2016 in Figure 2b) and other types of coal (Table 1). The slope of the regression of $E_{NO_x}^{CEMS}$ and $E_{CO_2}^{CEMS}$, $ratio_{regressed}^{CEMS}$, is assumed by setting the intercept to zero. Table 1 shows $ratio_{regressed,i,y}^{CEMS}$ by coal type and year.

https://doi.org/10.5194/acp-2019-521
Preprint. Discussion started: 8 July 2019

Atmospheric Chemistry and Physics Discussions

$ratio^{CEMS}_{regressed,i,y}$ will be applied to approximate $ratio^{CEMS}_{i,y}$ when estimating $E^{Sat}_{CO_2}$ from $E^{Sat}_{NO_x}$ for the 8 plants in Section 2.1 for years before post-combustion control systems were in operation.

$ratio^{CEMS}_{regressed}$ for power plants using bituminous coal decreased from 2005 (Figure 2a) to 2016 (Figure 2b) by 31% on average because of reductions in NO_x emission factors associated with improvements in boiler operations, such as by optimizing furnace design and operating conditions. The NO_x emissions factors, defined as NO_x emission rates per net electricity generation (Gg/TW h) declined by 33% from 2005 to 2016 (Figure 2c). We interpolate $ratio^{CEMS}_{regressed}$ to get year-specific ratios by coal type for the entire study period, as eGRID data are only available for some years (i.e., 2005, 2007, 2009, 2010, 2012, 2014 and 2016).

In addition, $ratio^{CEMS}_{regressed}$ shows significant variation by coal type and year (Figure 3). $ratio^{CEMS}_{regressed}$ is 1.7, 1.3 and 0.91 Gg NO_x/Tg CO_2 for bituminous, subbituminous and lignite coal in 2005, respectively. A reduction over time in $ratio^{CEMS}_{regressed}$ is observed for all coal types (Figure 3). $ratio^{CEMS}_{regressed}$ displays a large decrease of 31%, 36% and 20% from 2005 to 2016 for bituminous, subbituminous, and lignite coal, respectively.

2.2.2 Coal-fired power plants with post-combustion NO_x control systems

Here, we describe how we create continuous and consistent records of $ratio^{CEMS}$ for the entire study period for plants that had post-combustion NO_x control systems installed at some time during our study period, 2005–2017. The estimation is based on $ratio^{CEMS}_{regressed}$ derived in Section 2.2.1 for plants without post-combustion control systems in operation. We introduce a NO_x removal efficiency parameter, *f*, to adjust $ratio^{CEMS}_{regressed}$ for years after the installation of post-combustion control systems, $ratio^{CEMS-Estimated}$:

$$ratio^{CEMS-Estimated}_{i,y} = ratio^{CEMS}_{regressed,i,y} \times (1 - f_y)\,, \quad (2)$$

f is commonly measured for individual power plants to describe the performance of their post-combustion NO_x control systems. It is directly reported by some power plant databases, such as the China coal-fired Power plant Emissions Database (CPED; Liu et al., 2015). For databases that do not report *f*, like eGRID used in this study, one can estimate it for an individual power plant by first estimating the unabated emissions per electricity generation, $e_{unabated}$, which is the emission factor before the flue gas enters the post-combustion control system:

$$f_y = \frac{e_{unabated,y} - e_{CEMS,y}}{e_{unabated,y}}\,, \quad (3)$$

where e_{CEMS} denotes the actual emission factor in terms of CEMS NO_x emissions per net electricity generation (Gg/TW h). $e_{unabated}$ for a given year, $e_{unabated,y}$, is estimated based on the emission per electricity generation for years prior to, *p*, the installation of the post-combustion control system, $e_{unabated,p}$:

$$e_{unabated,y} = k_y \times e_{unabated,p}\,, \quad (4)$$

where the scaling factor, k_y, is used to account for the change over time in $e_{unabated}$ associated with improvements in boiler operations discussed in Section 2.2.1. k_y is calculated as the ratio of the averaged $e_{unabated}$ (i.e., the slope of the regression of NO_x emissions on electricity generation) in year, *t*, to that in year, *p*.

To assess the reliability of $ratio^{CEMS-Estimated}$, we select all power plants which had post-combustion devices installed between 2005 and 2016. Figure 4 shows a scatterplot of $ratio^{CEMS}$ (i.e., the ratio of $E^{CEMS}_{NO_x}$ to $E^{CEMS}_{CO_2}$ for individual plant) and $ratio^{CEMS-Estimated}$ for these power plants. We use the NO_x emissions factor in 2005, $e_{unabated,2005}$, to predict the unabated emission factor in 2016, $e_{unabated,2016}$, following Equations (3) and (4) in order to quantify the removal efficiencies for 2016, f_{2016}. $ratio^{CEMS-Estimated}_{2016}$ is based on the estimated f_{2016} and $ratio^{CEMS}_{regressed,2016}$ from Section 2.2.1. $ratio^{CEMS}$ and

https://doi.org/10.5194/acp-2019-521
Preprint. Discussion started: 8 July 2019

Atmospheric Chemistry and Physics Discussions

$ratio^{CEMS-Estimated}$ show good correlation (R^2 = 0.64), which increases our confidence that the estimated removal efficiencies approximate the actual efficiencies well. The slight underestimation suggested by the slope of 0.85 arises from the uncertainties in estimating unabated NO_x emission factors using Equation (4) and thus removal efficiencies, which is a major source of error (see details in Section 3.2) contributing to the overall uncertainties of $E_{CO_2}^{Sat}$.

3 Results and Discussion

In Section 3.1, we present $E_{CO_2}^{Sat}$ for our selected power plants and, in Section 3.2, discuss the uncertainties associated with $E_{CO_2}^{Sat}$. We apply the approach to power plants in South Africa in Section 3.3.

3.1 Satellite-derived CO_2 emissions ($E_{CO_2}^{Sat}$)

Figure 6a is a scatterplot of $E_{CO_2}^{Sat}$ and $E_{CO_2}^{CEMS}$ for the 8 power plants (Figure 5), 7 of which did not have post-combustion NO_x control systems installed during the study period, 2005–2017. The comparison shows a good correlation, R^2, of 0.66. $E_{CO_2}^{Sat}$ and $E_{CO_2}^{CEMS}$ for individual power plants are tabulated in Table 2 and their relative difference with CEMS measurements are listed in Table 3. The average $E_{CO_2}^{CEMS}$ for all power plants is 2.0 Gg/h and the average $E_{CO_2}^{Sat}$ is 1.8 Gg/h. The relative difference for individual 3-year means (defined as $(E_{CO_2}^{Sat} - E_{CO_2}^{CEMS})/E_{CO_2}^{CEMS}$) is 8% ± 41% (mean ± standard deviation). For example, Figure 1 shows $E_{CO_2}^{Sat}$ for the Rockport power plant, which typically has a positive bias as compared to $E_{CO_2}^{CEMS}$ because of a positive bias in $E_{NO_x}^{Sat}$.

The time series between $E_{CO_2}^{Sat}$ and $E_{CO_2}^{CEMS}$ are generally consistent, with their annual averages for the 8 power plants exhibiting a declining trend of 5%/yr and 3%/yr from 2006* to 2016* for $E_{CO_2}^{Sat}$ and $E_{CO_2}^{CEMS}$, respectively. The reduction in net electricity generation is the driving force underlying the emission changes, which has decreased by 37% for the 8 power plants from 2005 to 2016, as power producers shut down coal-fired units in favor of cheaper and more flexible natural gas as well as solar and wind (USEIA, 2018). It is interesting to note that the temporal variations in $E_{CO_2}^{Sat}$ are not as "smooth" as those in $E_{CO_2}^{CEMS}$, which results from fluctuations in $E_{NO_x}^{Sat}$. Such fluctuations are caused by uncertainties associated with $E_{NO_x}^{Sat}$ as discussed in Section 3.2. For example, changes in VCDs do not necessarily relate linearly with NO_x emissions (e.g., Figure 2 in Duncan et al., 2013) due to temporal variations in meteorology, and nonlinear NO_x chemistry (Valin et al, 2013) and transport. Averaging VCDs for a long-term period (3 years in this study) helps reduce those influences, but small fluctuations may still exist.

3.2 Uncertainties

We estimate the uncertainty of $E_{CO_2}^{Sat}$ based on the fit performance of $E_{NO_x}^{Sat}$ and comparison with $E_{CO_2}^{CEMS}$. The major sources of uncertainty include (a) the fitted NO_x lifetimes and $E_{NO_x}^{Sat}$ (Liu et al., 2016); (b) $ratio_{regressed}^{CEMS}$; and (c) f. We assume that their contributions to the total uncertainty are independent and define the total uncertainty as their root mean square.

(a) The uncertainty of the fitted NO_x lifetimes and $E_{NO_x}^{Sat}$ are quantified following the method described in Liu et al. (2017), accounting for errors arising from both the fit procedure and OMI NO_2 VCD observations (Liu et al., 2016). Particularly, the tropospheric air mass factors (AMF) used in NO_2 retrievals are based on relatively coarsely resolved surface albedo data and a priori NO_2 vertical profile shapes, likely causing low-biased VCDs over strong emission sources (e.g., Russell et al., 2011; McLinden et al., 2014; Griffin et al., 2019). The average AMF uncertainty of ~30% (see Table 2 in Boersma et al., 2007) likely contributes to the underestimation of emissions from some power plants in this study. Both random and systematic (bias) uncertainties in VCDs directly propagates into the uncertainty of $E_{NO_x}^{Sat}$ (see details in the supplement of Liu et al.

https://doi.org/10.5194/acp-2019-521
Preprint. Discussion started: 8 July 2019

Atmospheric Chemistry and Physics Discussions

(2016) and Section 3.4 of Liu et al. (2017)). The overall uncertainties of $E_{NO_x}^{Sat}$ range from 60% to 95% for all power plants in our analysis, which is comparable with the level of differences between $E_{NO_x}^{Sat}$ and $E_{NO_x}^{CEMS}$.

(b) For power plants without post-combustion devices, $ratio_{regressed}^{CEMS}$ derived from the regression (Figure 2a & b) and the plant-specific CEMS measurements are found to be within 15%, which is assumed as the uncertainty of the ratio to be applied to all power plants.

(c) For power plants with post-combustion devices, an additional uncertainty of 20% is applied to reflect the difference between the predicted and the true removal efficiency as suggested by Figure 4.

The overall uncertainties of $E_{CO_2}^{Sat}$ range from 62%–96% for the power plants in our analysis. However, it is worth noting that this uncertainty estimate is rather conservative. For power plants, relative differences between $E_{CO_2}^{CEMS}$ and $E_{CO_2}^{Sat}$ are 8% ±41% (mean ± standard deviation) (Figure 6a).

3.3 Application

We apply the approach proposed in this study to estimate CO_2 emissions from a power plant in South Africa, aiming to assess the capability of the approach to provide constraint on CO_2 emissions for regions outside the US. We chose South Africa, a country without reliable emissions accounting, as the area of interest, because we found available information on coal type and NO_x control status for its power plants. The power plant of Matimba (including the nearby Medupi which has operated since 2015) in South Africa are particularly suitable for application of our method, because it is a strong isolated NO_x point source (Figure 7). We estimate $E_{NO_x}^{Sat}$ for Matimba from 2005 to 2017 based on OMI NO_2 observations following the approach in Section 2.1. Matimba use subbituminous coal with the calorific value of ~ 20 MJ/kg (Makgato and Chirwa, 2017). We assume the NO_x to CO_2 emission ratio of Matimba is on the upper end of the US values, considering that it is not equipped with any NO_x control devices, even low-NO_x burners which are widely installed in US power plants (Pretorius et al., 2015). We thus use the ratio ranging from 2005 $ratio_{regressed}^{CEMS}$ to 2005 $ratio_{regressed}^{CEMS}$ + standard deviation for subbituminous coal listed in Table 1 to infer $E_{CO_2}^{Sat}$ based on $E_{NO_x}^{Sat}$. The derived $E_{CO_2}^{Sat}$ is shown in Figure 8 and fluctuates over time. Note that the range of $E_{CO_2}^{Sat}$ in Figure 8 represents the emissions based on a range of NO_x-to-CO_2 ratios, not the uncertainty. The overall uncertainty of $E_{CO_2}^{Sat}$ is ~70% for the Matimba power plant. The growth after 2008* is most likely caused by the increased unit operating hours driven by the desire to meet fully the demand for electricity in South Africa after a period of rolling blackouts (2007–2008) (Duncan et al., 2016). The decline afterwards may be associated with the tripping of generating units at the Matimba due to overload and the shortage of coal supply. The newly-built power plant of Medupi contributes to the increase from 2015*.

Figure 8 compares $E_{CO_2}^{Sat}$ derived in this study with other publicly available estimates and shows reasonable agreement. $E_{CO_2}^{Sat}$ falls between the estimates based on OCO-2 CO_2 observations (Nassar et al., 2017) and two bottom-up estimates including Wheeler and Ummel (2008) and Tong et al. (2018). We make a further comparison of NO_x emissions esttimates to Tong et al. (2018), the only database that reports both CO_2 and NO_x emissions, in order to shed light on the reason for the difference. The differences between $E_{NO_x}^{Sat}$ and bottom-up estimates contribute significantly to the differences of CO_2 estimates. $E_{NO_x}^{Sat}$ for Matimba is 3.8 Mg/h for 2010*, which is 65% smaller than the estimate by Tong et al. (2018) for 2010. It is not surprising to see such differences considering the uncertainties of satellite-derived NO_x emissions and bottom-up estimates without reliable CEMS measurements. On one hand, $E_{NO_x}^{Sat}$ is potentially underestimated, due to the bias in the OMI NO_2 standard product (version 3.1) associated with a low-resolution static climatology of surface Lambert-Equivalent Reflectivity (OMLER) (Kleipool et al., 2008). We perform a sensitivity analysis by using the preliminary new version OMI NO_2 product, which uses new geometry dependent MODIS-based surface reflectivity. The inferred $E_{NO_x}^{Sat}$ based on the new product increases by over 10%. On the other hand, the bottom-up estimates for Matimba are subject to significant uncertainties. For

https://doi.org/10.5194/acp-2019-521
Preprint. Discussion started: 8 July 2019

Atmospheric Chemistry and Physics Discussions

example, national total fuel consumption of the power sector for South Africa as reported by the International Energy Agency is used to estimate fuel consumption at the plant level as detailed fuel consumption for each plant is not currently available. Additionally, due to the absence of country-specific measurement data, default NO_x emission factors obtained from literature are applied (Tong et al., 2018).

4 Conclusions

We present a method to estimate CO_2 emissions of ozone season from individual power plants from satellite observations of co-emitted NO_2 and demonstrate its utility for US power plants, which have accurate CEMS with which to evaluate our method. While the uncertainty associated with our method is relatively high when applied to OMI data, we expect that the uncertainty will be less for the recently launched European Union Copernicus Sentinel 5 precursor (TROPOMI, launch October 2017), and the upcoming NASA geostationary Earth Venture one (TEMPO, launch expected in the early 2020s), both of which have superior capabilities. For example, higher spatiotemporal resolutions will likely improve the estimation of NO_x emissions as well as allow for the separation of more power plant plumes from nearby sources, thus increasing the number of power plants available for analysis. Therefore, future work will be to apply our method to these new datasets, especially after several years of vetted TROPOMI data become available.

We explore the feasibility of estimating CO_2 emissions from power plants in regions of the world without reliable emissions accounting by applying our method to a South African plant. The emissions estimates for the power plant of Matimba show reasonable agreement with existing estimates. The ratios derived in this study have the potential to be applied to power plants located in other regions by carefully investigating their coal type and NO_x control devices, in order to provide an additional constraint on CO_2 emissions. Future work will include applying our method to other regions of the world with reliable CEMS information, such as Europe, Canada and, more recently, China, to develop a more reliable and complete database with region-specific ratios. This method will also serve as an independent approach to check CO_2 emissions based on satellite retrievals of CO_2 average mixing ratio from future CO_2 sensors with improved accuracy and extended the spatial coverage (Bovensmann et al., 2010).

Author contribution

Fei Liu, Bryan N. Duncan, and Nickolay A. Krotkov designed the framework. Fei Liu, Steffen Beirle, Lok N. Lamsal, Debora Griffin, Chris A. McLinden, and Daniel L. Goldberg developed the NO_x emission fitting algorithm and Fei Liu carried it out. Fei Liu and Zifeng Lu analysed the NO_x/CO_2 emission ratio. Fei Liu and Bryan N. Duncan prepared the manuscript with contributions from all co-authors.

Acknowledgments

This research has been funded by the NASA's Earth Science Division Atmospheric Composition: Modeling and Analysis Program (ACMAP) and the Aura Science team. The Dutch-Finnish-built OMI instrument is part of the NASA EOS Aura satellite payload. KNMI and the Netherlands Space Agency (NSO) manage the OMI project. We thank the US EPA for making the Emissions & Generation Resource Integrated Database (eGRID) available on line.

References

Ackerman, K. V., and Sundquist, E. T.: Comparison of two U.S. power-plant carbon dioxide emissions data sets, Environ. Sci. Technol., 42, 5688–5693, doi: 10.1021/es800221q, 2008.

https://doi.org/10.5194/acp-2019-521
Preprint. Discussion started: 8 July 2019

Atmospheric Chemistry and Physics Discussions

1 Basu, S., Guerlet, S., Butz, A., Houweling, S., Hasekamp, O., Aben, I., Krummel, P., Steele, P., Langenfelds, R., Torn, M.,
2 Biraud, S., Stephens, B., Andrews, A., and Worthy, D.: Global CO_2 fluxes estimated from GOSAT retrievals of total column
3 CO_2, Atmos. Chem. Phys., 13, 8695–8717, doi: 10.5194/acp-13-8695-2013, 2013.
4 Beirle, S., Boersma, K. F., Platt, U., Lawrence, M. G., and Wagner, T.: Megacity emissions and lifetimes of nitrogen oxides
5 probed from space, Science, 333, 1737–1739, 2011.
6 Berezin, E. V., Konovalov, I. B., Ciais, P., Richter, A., Tao, S., Janssens-Maenhout, G., Beekmann, M., and Schulze, E. D.:
7 Multiannual changes of CO_2 emissions in China: indirect estimates derived from satellite measurements of tropospheric NO_2
8 columns, Atmos. Chem. Phys., 13, 9415–9438, doi: 10.5194/acp-13-9415-2013, 2013.
9 Boersma, K. F., Eskes, H. J., Dirksen, R. J., van der A, R. J., Veefkind, J. P., Stammes, P., Huijnen, V., Kleipool, Q. L.,
10 Sneep, M., Claas, J., Leitão, J., Richter, A., Zhou, Y., and Brunner, D.: An improved tropospheric NO_2 column retrieval
11 algorithm for the Ozone Monitoring Instrument, Atmos. Meas. Tech., 4, 1905–1928, doi:10.5194/amt-4-1905-2011, 2011.
12 Bovensmann, H., Buchwitz, M., Burrows, J. P., Reuter, M., Krings, T., Gerilowski, K., Schneising, O., Heymann, J.,
13 Tretner, A., and Erzinger, J.: A remote sensing technique for global monitoring of power plant CO_2 emissions from space
14 and related applications, Atmos. Meas. Tech., 3, 781–811, doi: 10.5194/amt-3-781-2010, 2010.
15 Buchwitz, M., Reuter, M., Schneising, O., Noël, S., Gier, B., Bovensmann, H., Burrows, J. P., Boesch, H., Anand, J., Parker,
16 R. J., Somkuti, P., Detmers, R. G., Hasekamp, O. P., Aben, I., Butz, A., Kuze, A., Suto, H., Yoshida, Y., Crisp, D., and
17 O'Dell, C.: Computation and analysis of atmospheric carbon dioxide annual mean growth rates from satellite observations
18 during 2003–2016, Atmos. Chem. Phys., 18, 17355–17370, doi: 10.5194/acp-18-17355-2018, 2018.
19 Burrows, J. P., Hölzle, E., Goede, A. P. H., Visser, H., and Fricke, W.: SCIAMACHY—scanning imaging absorption
20 spectrometer for atmospheric chartography, Acta Astronaut., 35, 445–451, doi: https://doi.org/10.1016/0094-5765(94)00278-
21 T, 1995.
22 Crisp, D.: Measuring atmospheric carbon dioxide from space with the Orbiting Carbon Observatory-2 (OCO-2), Proc. SPIE,
23 9607, 960702, doi: 10.1117/12.2187291, 2015.
24 de Foy, B., Lu, Z., Streets, D. G., Lamsal, L. N., and Duncan, B. N.: Estimates of power plant NO_x emissions and lifetimes
25 from OMI NO_2 satellite retrievals, Atmos. Environ., 116, 1–11, 2015.
26 Duncan, B. N., Yoshida, Y., de Foy, B., Lamsal, L. N., Streets, D. G., Lu, Z., Pickering, K. E., and Krotkov, N. A.: The
27 observed response of Ozone Monitoring Instrument (OMI) NO_2 columns to NO_x emission controls on power plants in the
28 United States: 2005–2011, Atmos. Environ., 81, 102–111, 2013.
29 Fioletov, V. E., McLinden, C. A., Krotkov, N., Moran, M. D., and Yang, K.: Estimation of SO_2 emissions using OMI
30 retrievals, Geophys. Res. Lett., 38, L21811, doi: 10.1029/2011gl049402, 2011.
31 Gelaro, R., McCarty, W., Suárez, M. J., Todling, R., Molod, A., Takacs, L., Randles, C. A., Darmenov, A., Bosilovich, M.
32 G., Reichle, R., Wargan, K., Coy, L., Cullather, R., Draper, C., Akella, S., Buchard, V., Conaty, A., Silva, A. M. d., Gu, W.,
33 Kim, G.-K., Koster, R., Lucchesi, R., Merkova, D., Nielsen, J. E., Partyka, G., Pawson, S., Putman, W., Rienecker, M.,
34 Schubert, S. D., Sienkiewicz, M., and Zhao, B.: The Modern-Era Retrospective Analysis for Research and Applications,
35 Version 2 (MERRA-2), J. Clim., 30, 5419–5454, doi: 10.1175/jcli-d-16-0758.1, 2017.
36 Glenn, C., Logan, T., Vu, B., Walsh, M., and Williams, P.: Evaluation of NOx Flue Gas Analyzers for Accuracy and Their
37 Applicability for Low-Concentration Measurements AU - Gluck, Steven, J. Air Waste Manage. Assoc., 53, 749–758, doi:
38 10.1080/10473289.2003.10466208, 2003.
39 Goldberg, D. L., Saide, P. E., Lamsal, L. N., de Foy, B., Lu, Z., Woo, J. H., Kim, Y., Kim, J., Gao, M., Carmichael, G., and
40 Streets, D. G.: A top-down assessment using OMI NO_2 suggests an underestimate in the NO_x emissions inventory in Seoul,
41 South Korea, during KORUS-AQ, Atmos. Chem. Phys., 19, 1801–1818, doi: 10.5194/acp-19-1801-2019, 2019.
42 Griffin, D., Zhao, X., McLinden, C. A., Boersma, F., Bourassa, A., Dammers, E., Degenstein, D., Eskes, H., Fehr, L.,
43 Fioletov, V., Hayden, K., Kharol, S. K., Li, S.-M., Makar, P., Martin, R. V., Mihele, C., Mittermeier, R. L., Krotkov, N.,

https://doi.org/10.5194/acp-2019-521
Preprint. Discussion started: 8 July 2019

Atmospheric Chemistry and Physics Discussions

Sneep, M., Lamsal, L. N., Linden, M. t., Geffen, J. v., Veefkind, P., and Wolde, M.: High-resolution mapping of nitrogen dioxide with TROPOMI: First results and validation over the Canadian oil sands, Geophys. Res. Lett., 46, 1049–1060, doi: 10.1029/2018gl081095, 2019.

Hakkarainen, J., Ialongo, I., and Tamminen, J.: Direct space-based observations of anthropogenic CO_2 emission areas from OCO-2, Geophys. Res. Lett., 43, 11,400–411,406, doi: 10.1002/2016GL070885, 2016.

Houweling, S., Baker, D., Basu, S., Boesch, H., Butz, A., Chevallier, F., Deng, F., Dlugokencky, E. J., Feng, L., Ganshin, A., Hasekamp, O., Jones, D., Maksyutov, S., Marshall, J., Oda, T., O'Dell, C. W., Oshchepkov, S., Palmer, P. I., Peylin, P., Poussi, Z., Reum, F., Takagi, H., Yoshida, Y., and Zhuravlev, R.: An intercomparison of inverse models for estimating sources and sinks of CO_2 using GOSAT measurements, Journal of Geophysical Research: Atmospheres, 120, 5253–5266, doi:10.1002/2014JD022962, 2015.

Janardanan, R., Maksyutov, S., Oda, T., Saito, M., Kaiser, J. W., Ganshin, A., Stohl, A., Matsunaga, T., Yoshida, Y., and Yokota, T.: Comparing GOSAT observations of localized CO_2 enhancements by large emitters with inventory-based estimates, Geophys. Res. Lett., 43, 3486–3493, doi: 10.1002/2016GL067843, 2016.

Janssens-Maenhout, G., Crippa, M., Guizzardi, D., Muntean, M., Schaaf, E., Dentener, F., Bergamaschi, P., Pagliari, V., Olivier, J. G. J., Peters, J. A. H. W., van Aardenne, J. A., Monni, S., Doering, U., and Petrescu, A. M. R.: EDGAR v4.3.2 global atlas of the three major greenhouse gas emissions for the period 1970–2012, Earth Syst. Sci. Data Discuss., 2017, 1–55, doi: 10.5194/essd-2017-79, 2017.

Kleipool, Q. L., Dobber, M. R., de Haan, J. F., and Levelt, P. F.: Earth surface reflectance climatology from 3 years of OMI data, Journal of Geophysical Research: Atmospheres, 113, doi: 10.1029/2008jd010290, 2008.

Konovalov, I. B., Berezin, E. V., Ciais, P., Broquet, G., Zhuravlev, R. V., and Janssens-Maenhout, G.: Estimation of fossil-fuel CO_2 emissions using satellite measurements of "proxy" species, Atmos. Chem. Phys., 16, 13509–13540, doi:10.5194/acp-16-13509-2016, 2016.

Kort, E. A., Frankenberg, C., Miller, C. E., and Oda, T.: Space-based observations of megacity carbon dioxide, Geophys. Res. Lett., 39, L17806, doi: 10.1029/2012GL052738, 2012.

Krotkov, N. A., Lamsal, L. N., Celarier, E. A., Swartz, W. H., Marchenko, S. V., Bucsela, E. J., Chan, K. L., Wenig, M., and Zara, M.: The version 3 OMI NO_2 standard product, Atmos. Meas. Tech., 10, 3133–3149, doi: 10.5194/amt-10-3133-2017, 2017.

Levelt, P. F., van den Oord, G. H. J., Dobber, M. R., Malkki, A., Huib, V., Johan de, V., Stammes, P., Lundell, J. O. V., and Saari, H.: The ozone monitoring instrument, Geoscience and Remote Sensing, IEEE Transactions on, 44, 1093–1101, 2006.

Levelt, P. F., Joiner, J., Tamminen, J., Veefkind, J. P., Bhartia, P. K., Stein Zweers, D. C., Duncan, B. N., Streets, D. G., Eskes, H., van der A, R., McLinden, C., Fioletov, V., Carn, S., de Laat, J., DeLand, M., Marchenko, S., McPeters, R., Ziemke, J., Fu, D., Liu, X., Pickering, K., Apituley, A., González Abad, G., Arola, A., Boersma, F., Chan Miller, C., Chance, K., de Graaf, M., Hakkarainen, J., Hassinen, S., Ialongo, I., Kleipool, Q., Krotkov, N., Li, C., Lamsal, L., Newman, P., Nowlan, C., Suleiman, R., Tilstra, L. G., Torres, O., Wang, H., and Wargan, K.: The Ozone Monitoring Instrument: overview of 14 years in space, Atmos. Chem. Phys., 18, 5699–5745, doi: 10.5194/acp-18-5699-2018, 2018.

Liu, F., Zhang, Q., Tong, D., Zheng, B., Li, M., Huo, H., and He, K. B.: High-resolution inventory of technologies, activities, and emissions of coal-fired power plants in China from 1990 to 2010, Atmos. Chem. Phys., 15, 13299–13317, doi: 10.5194/acp-15-13299-2015, 2015.

Liu, F., Beirle, S., Zhang, Q., Dörner, S., He, K., and Wagner, T.: NO_x lifetimes and emissions of cities and power plants in polluted background estimated by satellite observations, Atmos. Chem. Phys., 16, 5283–5298, doi: 10.5194/acp-16-5283-2016, 2016.

https://doi.org/10.5194/acp-2019-521
Preprint. Discussion started: 8 July 2019

Atmospheric Chemistry and Physics Discussions

1 Liu, F., Beirle, S., Zhang, Q., van der A, R. J., Zheng, B., Tong, D., and He, K.: NO_x emission trends over Chinese cities
2 estimated from OMI observations during 2005 to 2015, Atmos. Chem. Phys., 17, 9261–9275, doi: 10.5194/acp-17-9261-
3 2017, 2017.
4 Lu, Z., and Streets, D. G.: Increase in NO_x emissions from Indian thermal power plants during 1996–2010: Unit-based
5 inventories and multisatellite observations, Environ. Sci. Technol., 46, 7463–7470, doi: 10.1021/es300831w, 2012.
6 Lu, Z., Streets, D. G., de Foy, B., and Krotkov, N. A.: Ozone Monitoring Instrument observations of interannual increases in
7 SO_2 emissions from Indian coal-fired power plants during 2005–2012, Environ. Sci. Technol., 47, 13993–14000, 2013.
8 Lu, Z., Streets, D. G., de Foy, B., Lamsal, L. N., Duncan, B. N., and Xing, J.: Emissions of nitrogen oxides from US urban
9 areas: estimation from Ozone Monitoring Instrument retrievals for 2005–2014, Atmos. Chem. Phys., 15, 10367–10383, doi:
10 10.5194/acp-15-10367-2015, 2015.
11 Majanne, Y., Korpela, T., Judl, J., Koskela, S., Laukkanen, V., and Häyrinen, A.: Real Time Monitoring of Environmental
12 Efficiency of Power Plants, IFAC-PapersOnLine, 48, 495–500, doi: https://doi.org/10.1016/j.ifacol.2015.12.428, 2015.
13 Makgato, S., and Chirwa, E.: Characteristics of Thermal Coal used by Power Plants in Waterberg Region of South Africa,
14 Chemical Engineering Transactions, 57, 511–516, 10.3303/CET1757086, 2017.
15 McLinden, C. A., Fioletov, V., Boersma, K. F., Kharol, S. K., Krotkov, N., Lamsal, L., Makar, P. A., Martin, R. V.,
16 Veefkind, J. P., and Yang, K.: Improved satellite retrievals of NO_2 and SO_2 over the Canadian oil sands and comparisons
17 with surface measurements, Atmos. Chem. Phys., 14, 3637–3656, doi: 10.5194/acp-14-3637-2014, 2014.
18 Nassar, R., Hill, T. G., McLinden, C. A., Wunch, D., Jones, D. B. A., and Crisp, D.: Quantifying CO_2 Emissions From
19 Individual Power Plants From Space, Geophys. Res. Lett., 44, 10,045–010,053, doi:10.1002/2017GL074702, 2017.
20 Pretorius, I., Piketh, S., Burger, R., and Neomagus, H.: A perspective on South African coal fired power station emissions,
21 Journal of Energy in Southern Africa, 26, 27–40, doi: 10.17159/2413-3051/2015/v26i3a2127, 2015.
22 Reuter, M., Buchwitz, M., Hilboll, A., Richter, A., Schneising, O., Hilker, M., Heymann, J., Bovensmann, H., and Burrows,
23 J. P.: Decreasing emissions of NO_x relative to CO_2 in East Asia inferred from satellite observations, Nature Geoscience, 7,
24 792, doi: 10.1038/ngeo2257, 2014.
25 Reuter, M., Buchwitz, M., Schneising, O., Krautwurst, S., O'Dell, C. W., Richter, A., Bovensmann, H., and Burrows, J. P.:
26 Towards monitoring localized CO2 emissions from space: co-located regional CO_2 and NO_2 enhancements observed by the
27 OCO-2 and S5P satellites, Atmos. Chem. Phys. Discuss., doi:10.5194/acp-2019-15, in review, 2019.
28 Russell, A. R., Perring, A. E., Valin, L. C., Bucsela, E. J., Browne, E. C., Wooldridge, P. J., and Cohen, R. C.: A high spatial
29 resolution retrieval of NO_2 column densities from OMI: method and evaluation, Atmos. Chem. Phys., 11, 8543–8554, doi:
30 10.5194/acp-11-8543-2011, 2011.
31 Schneising, O., Heymann, J., Buchwitz, M., Reuter, M., Bovensmann, H., and Burrows, J. P.: Anthropogenic carbon dioxide
32 source areas observed from space: assessment of regional enhancements and trends, Atmos. Chem. Phys., 13, 2445–2454,
33 doi: 10.5194/acp-13-2445-2013, 2013.
34 Schoeberl, M. R., Douglass, A. R., Hilsenrath, E., Bhartia, P. K., Beer, R., Waters, J. W., Gunson, M. R., Froidevaux, L.,
35 Gille, J. C., and Barnett, J. J.: Overview of the EOS Aura mission, Geoscience and Remote Sensing, IEEE Transactions on,
36 44, 1066–1074, 2006.
37 Shindell, D., and Faluvegi, G.: The net climate impact of coal-fired power plant emissions, Atmos. Chem. Phys., 10, 3247–
38 3260, doi: 10.5194/acp-10-3247-2010, 2010.
39 Tong, D., Zhang, Q., Davis, S. J., Liu, F., Zheng, B., Geng, G., Xue, T., Li, M., Hong, C., Lu, Z., Streets, D. G., Guan, D.,
40 and He, K.: Targeted emission reductions from global super-polluting power plant units, Nature Sustainability, 1, 59–68, doi:
41 10.1038/s41893-017-0003-y, 2018.
42 U.S. Energy Information Administration (USEIA), Electric Power Annual 2017, available at
43 https://www.eia.gov/electricity/annual/pdf/epa.pdf (last access: April 11, 2019), 2018.

https://doi.org/10.5194/acp-2019-521
Preprint. Discussion started: 8 July 2019

Atmospheric Chemistry and Physics Discussions

U.S. Environmental Protection Agency (USEPA), Compilation of Air Pollutant Emission Factors, AP-42, Fifth Edition, Volume 1, Chapter 1, Washington, D. C., available at: https://www3.epa.gov/ttn/chief/ap42/ch01/index.html (last access: March 20, 2019), 2009.

U.S. Environmental Protection Agency (USEPA): Technical support document for eGRID with year 2016 data (the Emissions & Generation Resource Integrated Database), Washington, D.C., 2018.

Valin, L. C., Russell, A. R., and Cohen, R. C.: Variations of OH radical in an urban plume inferred from NO_2 column measurements, Geophys. Res. Lett., 40, 1856–1860, doi:10.1002/grl.50267, 2013.

Veefkind, J. P., Aben, I., McMullan, K., Förster, H., de Vries, J., Otter, G., Claas, J., Eskes, H. J., de Haan, J. F., Kleipool, Q., van Weele, M., Hasekamp, O., Hoogeveen, R., Landgraf, J., Snel, R., Tol, P., Ingmann, P., Voors, R., Kruizinga, B., Vink, R., Visser, H., and Levelt, P. F.: TROPOMI on the ESA Sentinel-5 Precursor: A GMES mission for global observations of the atmospheric composition for climate, air quality and ozone layer applications, Remote Sens. Environ., 120, 70–83, 2012.

Velazco, V. A., Buchwitz, M., Bovensmann, H., Reuter, M., Schneising, O., Heymann, J., Krings, T., Gerilowski, K., and Burrows, J. P.: Towards space based verification of CO_2 emissions from strong localized sources: fossil fuel power plant emissions as seen by a CarbonSat constellation, Atmos. Meas. Tech., 4, 2809–2822, doi: 10.5194/amt-4-2809-2011, 2011.

Wheeler, D., and Ummel, K.: Calculating CARMA: Global estimation of CO_2 emissions from the power sector, Center for Global Development, Working Paper 145, 2008.

Yokota, T., Yoshida, Y., Eguchi, N., Ota, Y., Tanaka, T., Watanabe, H., and Maksyutov, S.: Global Concentrations of CO_2 and CH_4 Retrieved from GOSAT: First Preliminary Results, SOLA, 5, 160–163, doi: 10.2151/sola.2009-041, 2009.

https://doi.org/10.5194/acp-2019-521
Preprint. Discussion started: 8 July 2019

Atmospheric Chemistry and Physics Discussions

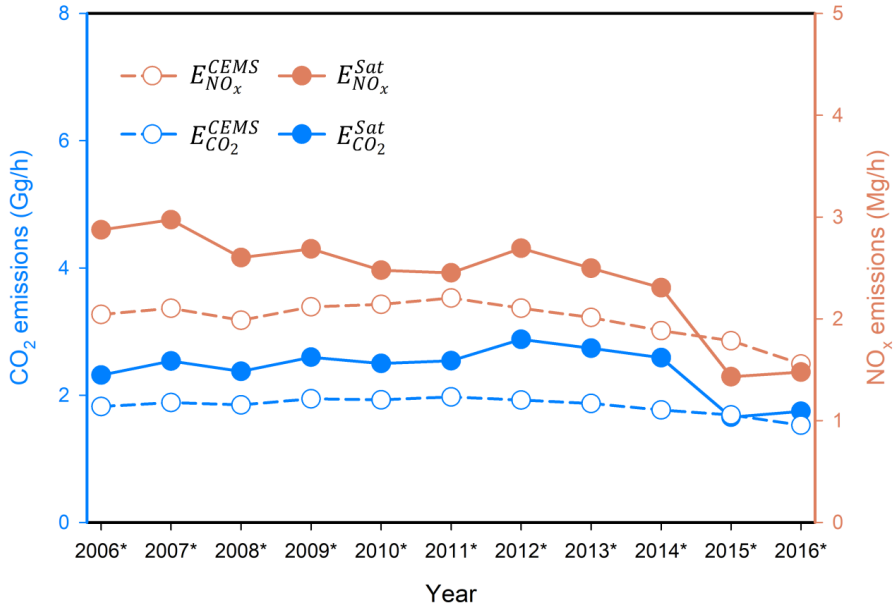

Figure 1 $E_{NO_x}^{Sat}$ (Mg/h; orange solid lines – right axis) and $E_{CO_2}^{Sat}$ (Gg/h; blue solid line – left axis) for the Rockport power plant (Indiana) during 2005 to 2017. $E_{NO_x}^{CEMS}$ and $E_{CO_2}^{CEMS}$ (dashed lines) are also shown. The 3-year periods are represented by the middle year with an asterisk (e.g., 2006* denotes the period from 2005 to 2007).

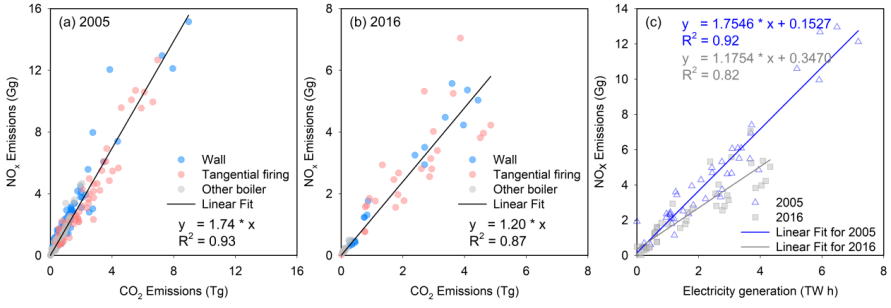

Figure 2 Scatter plots of $E_{NO_x}^{CEMS}$ versus $E_{CO_2}^{CEMS}$ for bituminous coal-fired electric generating units for (a) 2005 and (b) 2016. Values are color coded by firing type. (c) Scatter plot of $E_{NO_x}^{CEMS}$ versus electricity generation of the same units for years 2005 (triangle) and 2016 (square). Only plants without post-combustion NO_x control devices within a given year are used. The electricity generation data are also from eGRID. The lines in all three panels represent the computed linear regressions.

https://doi.org/10.5194/acp-2019-521
Preprint. Discussion started: 8 July 2019

Atmospheric Chemistry and Physics Discussions

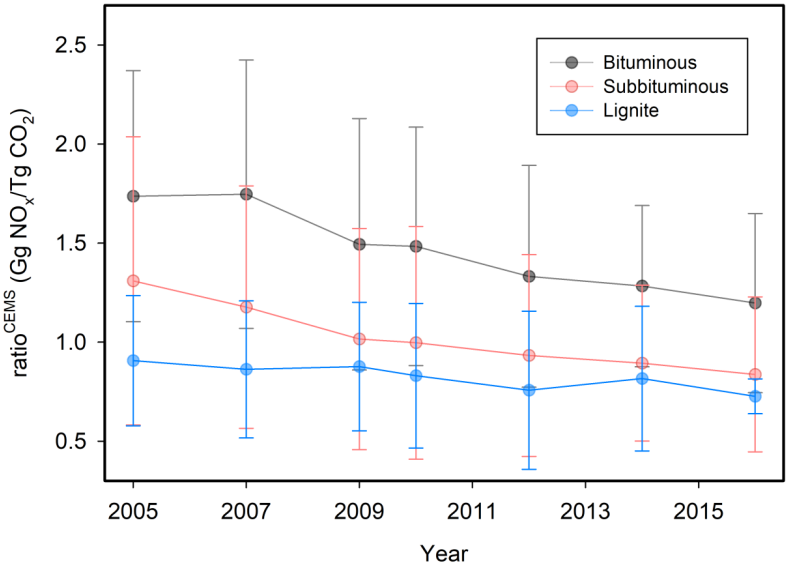

Figure 3 Interannual trends of $ratio^{CEMS}_{regressed}$ for power plants using bituminous, subbituminous and lignite coal types and without post-combustion NO_x control devices in a given year. Error bars show the standard deviations for ratios of $E^{CEMS}_{NO_x}$ to $E^{CEMS}_{CO_2}$ for individual power plants.

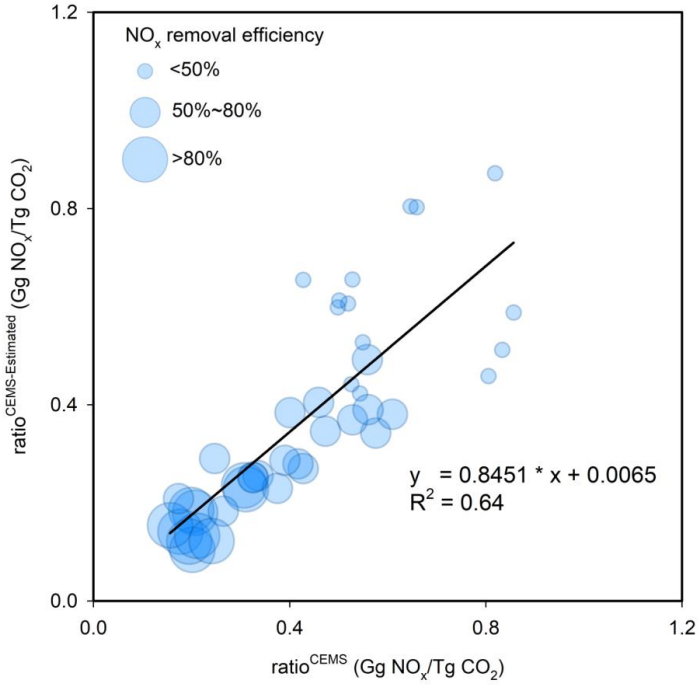

Figure 4 Scatterplot of the ratio of $ratio^{CEMS-Estimated}$ as compared to $ratio^{CEMS}$ for 2016. All coal-fired power plants that operated post-combustion techniques after 2005 and before 2016 are used in the plot. The sizes of the circles denote the magnitude of the NO_x reduction efficiency of post-combustion control devices estimated in this study. The line represents the linear regression of $ratio^{CEMS}$ to $ratio^{CEMS-Estimated}$.

https://doi.org/10.5194/acp-2019-521
Preprint. Discussion started: 8 July 2019

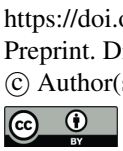

Atmospheric Chemistry and Physics Discussions

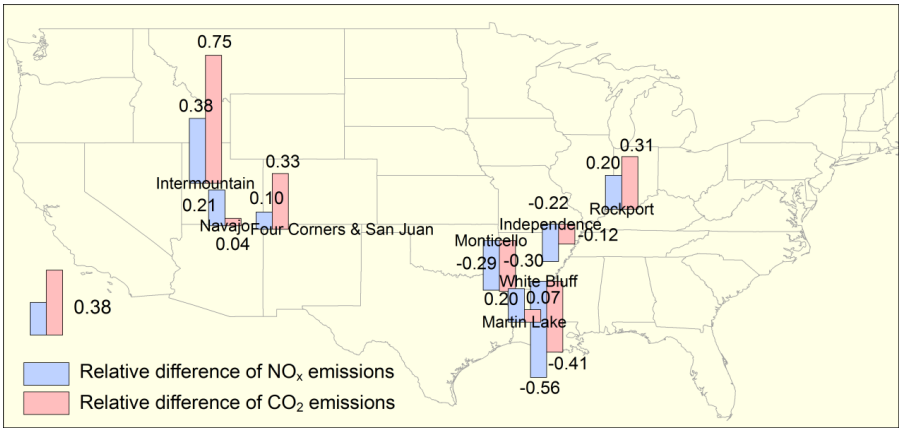

Figure 5 Locations of the investigated power plants in this study. The bar charts denote the relative differences, defined as (E^{Sat}–E^{CEMS})/E^{CEMS}, averaged over 2005–2017, for NO_x (blue) and CO_2 (red) emissions. The upward and downward bars represent positive and negative differences, respectively. The Monticello power plant installed SNCR to control NO_x emissions in 2008. Other power plants are not equipped with post-combustion NO_x control devices.

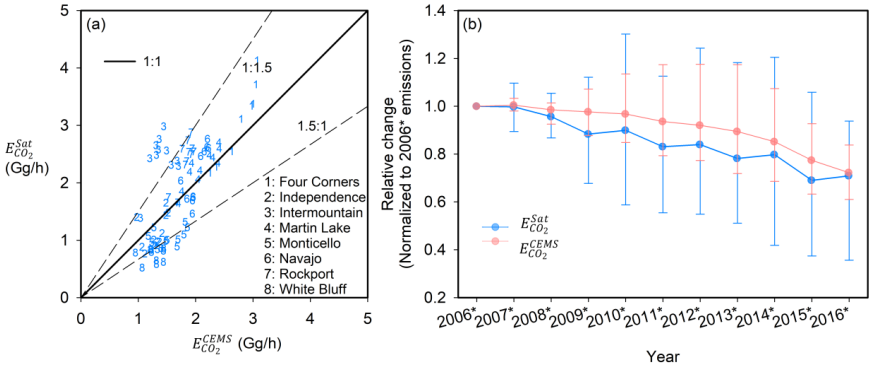

Figure 6 (a) Scatterplot of $E^{Sat}_{CO_2}$ for 8 power plants as compared to $E^{CEMS}_{CO_2}$ from 2006* to 2016*. The straight solid and dash lines represent the ratio of 1:1 and 1:1.5, respectively. (b) Interannual trends of the averaged $E^{Sat}_{CO_2}$ (blue lines) and $E^{CEMS}_{CO_2}$ (pink lines) is for all power plants analyzed in this study from 2006*–2016*, normalized to the 2006* value. The whiskers denote the maximum and minimum values.

https://doi.org/10.5194/acp-2019-521
Preprint. Discussion started: 8 July 2019

Atmospheric Chemistry and Physics Discussions

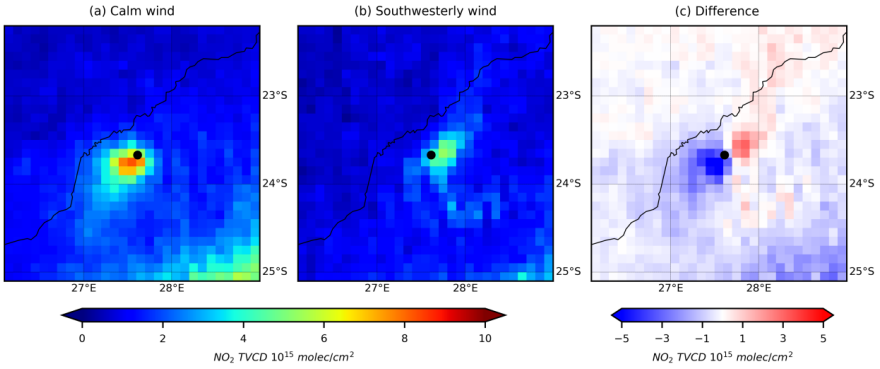

Figure 7 Mean OMI NO_2 TVCDs around the Matimba power plant (Lephalale, South Africa) for (a) calm, (b) southwesterly wind conditions and (c) their difference (southwesterly − calm) for the period of 2005 – 2017. The location of Matimba is labelled by a black dot.

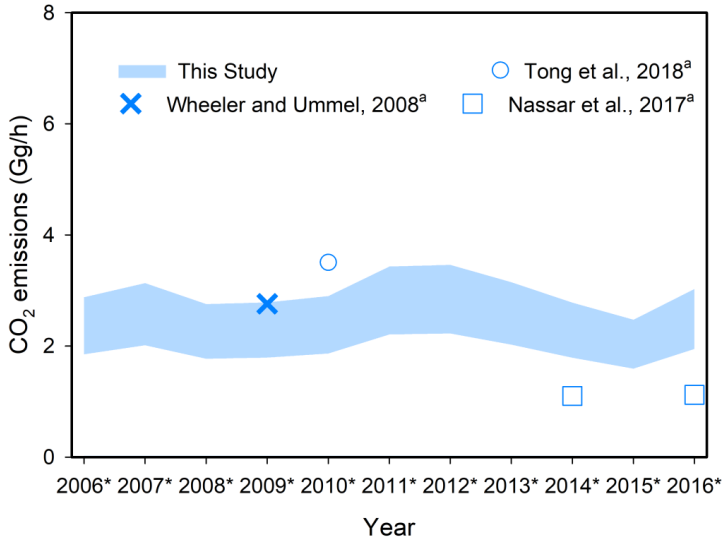

Figure 8 Comparison of $E_{CO_2}^{Sat}$ (Gg/h) derived in this study with existing estimates for the Matimba power plant during 2005 to 2017. $E_{CO_2}^{Sat}$ is inferred based on the NO_x to CO_2 emissions ratio ranging from $ratio_{regressed}^{CEMS}$ to $ratio_{regressed}^{CEMS}$ + standard deviation of ratio.

[a]Emissions are estimated for 2009 by Wheeler and Ummel (2008); for 2010 by Tong et al. (2018); and for 2014 and 2016 by Nassar at al. (2017).

https://doi.org/10.5194/acp-2019-521
Preprint. Discussion started: 8 July 2019

Atmospheric Chemistry and Physics Discussions

Table 1 The slope ($ratio_{regressed}^{CEMS}$), coefficient of determination, standard deviation and sample number of the linear regression of $E_{NO_x}^{CEMS}$ and $E_{CO_2}^{CEMS}$ by year for all US power plants without post-combustion NO_x control devices from 2005 to 2016.

Coal type	Year	$ratio_{regressed}^{CEMS}$	R^2	Standard deviation	Sample number[a]
Bituminous	2005	1.74	0.93	0.63	278
	2007	1.75	0.91	0.68	286
	2009	1.49	0.88	0.64	241
	2010	1.48	0.86	0.60	235
	2012	1.33	0.87	0.56	190
	2014	1.28	0.87	0.41	136
	2016	1.20	0.87	0.45	66
Subbituminous	2005	1.31	0.65	0.73	226
	2007	1.18	0.61	0.61	221
	2009	1.02	0.66	0.56	230
	2010	1.00	0.67	0.59	216
	2012	0.93	0.74	0.51	200
	2014	0.89	0.74	0.39	165
	2016	0.84	0.70	0.39	111
Lignite	2005	0.91	0.74	0.33	20
	2007	0.86	0.82	0.35	22
	2009	0.88	0.91	0.32	16
	2010	0.83	0.94	0.37	18
	2012	0.76	0.91	0.40	15
	2014	0.82	0.92	0.37	12
	2016	0.73	0.78	0.09	9

[a]The sample number generally decreases from 2005 to 2016 as power plants installed post-combustion NO_x control devices over time.

https://doi.org/10.5194/acp-2019-521
Preprint. Discussion started: 8 July 2019

Atmospheric Chemistry and Physics Discussions

Table 2 Summary of effective NO_x lifetimes, satellite-derived NO_x emissions ($E_{NO_x}^{Sat}$), CO_2 emissions ($E_{CO_2}^{Sat}$) and bottom-up NO_x emissions ($E_{NO_x}^{CEMS}$), CO_2 emissions ($E_{CO_2}^{CEMS}$) for 8 US power plants during May to September from 2005 to 2017. The 3-year periods are represented by the middle year with an asterisk.

Category	Year	Four Corners & San Juan	Independence	Intermountain	Martin Lake	Monticello	Navajo	Rockport	White Bluff
NO_x lifetime	2005-2017	2.7	2.5	2.2	2.3	3.2	2.3	2.4	4.3
	2006*	10.5	2.0	4.0	2.4	1.1	4.6	2.9	1.0
	2007*	10.0	1.7	4.1	2.3	1.1	4.4	3.0	0.9
	2008*	9.4	1.6	3.7	2.0	0.8	4.5	2.6	0.9
	2009*	7.2	1.2	3.9	2.1	0.7	3.9	2.7	0.7
$E_{NO_x}^{Sat}$	2010*	6.8	1.0	4.4	2.1	0.6	3.6	2.5	0.9
(Mg/h)	2011*	6.5	0.9	3.6	1.8	0.7	2.5	2.5	0.8
	2012*	6.3	0.9	3.4	1.6	0.6	2.3	2.7	0.8
	2013*	5.6	0.8	3.5	1.8	0.5	1.9	2.5	0.6
	2014*	4.4	0.7	3.5	1.7	0.8	2.2	2.3	0.5
	2015*	3.8	0.8	3.0	1.4	0.7	2.1	1.4	0.4
	2016*	3.5	1.2	1.7	1.2	0.6	2.5	1.5	0.7
	2006*	7.4	1.8	3.0	1.8	1.5	3.8	2.0	1.7
	2007*	7.3	1.8	3.1	1.8	1.4	3.9	2.1	1.6
	2008*	6.8	1.8	2.9	1.8	1.3	3.8	2.0	1.6
	2009*	6.5	1.6	2.9	1.8	1.2	3.4	2.1	1.8
$E_{NO_x}^{CEMS}$	2010*	6.2	1.6	2.8	1.7	1.1	2.8	2.1	1.8
(Mg/h)	2011*	6.2	1.4	2.5	1.5	1.0	2.2	2.2	1.9
	2012*	6.1	1.3	2.4	1.4	0.9	1.9	2.1	1.9
	2013*	5.6	1.3	2.4	1.3	0.9	1.9	2.0	2.0
	2014*	5.2	1.2	2.5	1.3	0.8	1.9	1.9	1.9
	2015*	4.3	1.2	2.0	1.3	0.8	1.7	1.8	1.5
	2016*	3.9	1.1	1.5	1.2	0.8	1.6	1.6	1.2
$(E_{NO_x}^{Sat} - E_{NO_x}^{CEMS}) / E_{NO_x}^{CEMS}$	2005-2017	10%	-22%	38%	20%	-29%	21%	20%	-56%
	2006*	6.1	1.6	2.3	2.7	1.2	2.6	2.3	0.8
	2007*	5.9	1.5	2.4	2.6	1.3	2.6	2.5	0.8
	2008*	5.6	1.4	2.3	2.3	1.1	2.8	2.4	0.8
	2009*	4.1	1.1	2.6	2.4	1.0	2.5	2.6	0.6
$E_{CO_2}^{Sat}$	2010*	3.7	1.0	3.0	2.5	0.9	2.5	2.5	0.9
(Gg/h)	2011*	3.4	1.0	2.6	2.2	1.0	1.7	2.5	0.8
	2012*	3.3	1.0	2.5	2.1	1.0	1.7	2.9	0.9
	2013*	3.1	0.9	2.6	2.3	0.8	1.5	2.7	0.6
	2014*	2.5	0.8	2.8	2.2	1.2	1.8	2.6	0.6
	2015*	2.3	0.9	2.4	1.8	1.1	1.7	1.7	0.5
	2016*	2.2	1.4	1.4	1.6	1.0	2.0	1.7	0.8
	2006*	3.1	1.5	1.7	2.4	1.9	2.2	1.8	1.2
	2007*	3.1	1.5	1.7	2.4	1.8	2.2	1.9	1.2
	2008*	3.0	1.5	1.6	2.4	1.8	2.2	1.8	1.2
	2009*	3.1	1.4	1.5	2.3	1.7	2.1	1.9	1.3
$E_{CO_2}^{CEMS}$	2010*	3.0	1.4	1.4	2.2	1.7	2.1	1.9	1.4
(Gg/h)	2011*	3.0	1.3	1.3	2.1	1.5	2.0	2.0	1.4

https://doi.org/10.5194/acp-2019-521
Preprint. Discussion started: 8 July 2019

Atmospheric Chemistry and Physics Discussions

	2012*	3.0	1.3	1.3	2.0	1.5	1.9	1.9	1.4
	2013*	2.8	1.3	1.3	1.9	1.3	1.9	1.9	1.4
	2014*	2.6	1.1	1.4	1.9	1.3	2.0	1.8	1.3
	2015*	2.4	1.1	1.2	1.8	1.2	1.8	1.7	1.1
	2016*	2.2	1.0	1.0	1.7	1.2	1.7	1.5	0.9
$(E_{CO_2}^{Sat} - E_{CO_2}^{CEMS}) / E_{CO_2}^{CEMS}$	2005-2017	33%	-12%	75%	7%	-30%	4%	31%	-41%

https://doi.org/10.5194/acp-2019-521
Preprint. Discussion started: 8 July 2019

Atmospheric Chemistry and Physics Discussions

Table 3 Summary of relative difference between satellite-derived NO_x emissions ($E_{NO_x}^{Sat}$) and bottom-up NO_x emissions ($E_{NO_x}^{CEMS}$), satellite-derived CO_2 emissions ($E_{CO_2}^{Sat}$) and bottom-up CO_2 emissions ($E_{CO_2}^{CEMS}$) for 8 US power plants during May to September from 2005 to 2017. The 3-year periods are represented by the middle year with an asterisk.

Year	NO_x		CO_2	
	Mean	Standard Deviation	Mean	Standard Deviation
2006*	15%	29%	17%	39%
2007*	10%	29%	16%	38%
2008*	5%	30%	14%	39%
2009*	-3%	34%	6%	39%
2010*	-1%	38%	9%	46%
2011*	-5%	31%	3%	40%
2012*	-3%	31%	5%	41%
2013*	-4%	38%	4%	49%
2014*	-3%	36%	7%	46%
2015*	-8%	35%	2%	41%
2016*	-2%	29%	8%	22%